Climate Change Edition

Influence of Operating Conditions on Deposition Rate and Smoothness of Electrolytic Aluminum Foil Using Chloroaluminate Ionic Liquids*

Koichi Ui**, Satoshi Kobayashi***, Kuniaki Sasaki****, Tatsuya Takeguchi**, Tetsuya Tsuda*****, Mikito Ueda******, Junji Nunomura*******, Yukio Honkawa******** and Yoichi Kojima*********

The ionic liquid comprised of anhydrous aluminum chloride ($AlCl_3$) and 1-ethyl-3-methylimidazolium chloride (EMIC) has attracted attention as an electrolyte for Al electrolysis. We have investigated the influence of the operating conditions on the deposition rate and the surface roughness of electrolytic Al foil by using the $AlCl_3$-EMIC melt with/without 20 mmol dm^{-3} of an 1, 10-phenanthroline anhydrate (OP) additive as the electrolyte. The cross-sectional SIM images revealed that the increase in the operating temperature affected the foil thickness and the OP addition affected the smoothness. At the operating temperature of 50 ℃ and the current density of 52.6 mA cm^{-2}, the current efficiency was 90% or more and the deposition rate was about 0.9 μm min^{-1} regardless of the OP addition. An AFM image revealed that the surface roughness value of the Al foil obtained on the Ti plate substrate from the melt with the OP additive at 50 ℃ was 45.8 nm at the current density of 52.6 mA cm^{-2}. The XRD patterns showed that the orientations of the (200) reflections became strong by the OP addition. A smooth Al foil was obtained even at a high current density by increasing the operating temperature and adding OP to the melt.

Keywords: *Electrodeposition, Aluminum, Ionic liquid, Aluminum chloride, 1-ethyl-3-methylimidazolium chloride*

1. Introduction

Aluminum (Al), along with iron (Fe) and copper (Cu), is one of the indispensable materials in our life[1]. Al is not expensive and has a specific gravity of about one-third that of Fe. In addition, it is relatively soft and has a high malleability, which has the property of being easily processed into various shapes. Therefore, it has been adopted in various products. Al foil is one of the products that takes advantage of these properties, which has been used for various purposes. In particular, electrical equipment applications mainly include electrode foils for Al electrolytic capacitors and the current collectors for the positive electrodes of lithium-ion batteries (LIBs). In the Cu foil of the current collector for the negative electrodes of LIBs, a rolling method or an electrolysis method is used depending on the applications and the required characteristics[2, 3]. On the other hand, whereas Al foil is industrially manufactured by the rolling method, the production of Al foil by the electrolytic method (electrolytic Al foil) has not yet been established.

One of the reasons for this is that the standard electrode potential of Al (−1.676 V *vs.* SHE) is much lower than that of hydrogen, which makes it difficult to electrodeposit Al from aqueous solutions. Non-

* This paper has been published in Journal of The Electrochemical Society, **168** (2021), 056510.
** Faculty of Science and Engineering, Iwate University, Dr. Eng.
*** Nippon Light Metal Company, Ltd., Formerly Graduate School of Engineering, Iwate University.
**** Technical Division, Iwate University.
***** Faculty of Engineering, Chiba University, Dr. Energy Science.
****** Faculty of Engineering, Hokkaido University, Dr. Eng.
******* Research Department I, Research & Development Center, Marketing & Technology Division, UACJ Corporation/Faculty of Engineering, Hokkaido University.
******** Climate Change Task Force Department, Corporate Sustainability Division, UACJ Corporation.
********* Research & Development Center, Marketing & Technology Division, UACJ Corporation, Ph. D.

aqueous solutions, such as molten salts[4 ~ 8], ionic liquids (ILs)[9 ~ 14], and organic solvents[2, 3, 15], have been used as the electrolytes for the electrodeposition of Al at ambient temperature. In addition, in recent years, deep eutectic solvents have also been studied as the electrolytes[16, 17], all of which are at the stage of basic research. When these liquids are employed, electrodeposition is required in an atmosphere of an inert gas and the solution cost is higher than that of using an aqueous solution. Thus, the production of Al foils by the electrolytic method has several problems in terms of safety, cost, and technology, thus it has not yet been widely put into practical use[3].

In the case of electrolytic Cu foil, its properties are governed by the operating conditions of the electrolysis[18]. In general, the operating conditions (metal ion concentration, additives, current density, temperature, agitation, polarization) will determine the grain sizes of the deposits.[19] These conditions affect the grain size of the electrolytic Cu foil that determines the deposition rate and the surface roughness (smoothness). Similarly, the production of Al foil will require these conditions. The physical properties of Al foils will require the deposition rate and smoothness as the first step. In the articles on Al electrodeposition using ILs, the relation between the operating conditions and the smoothness has been reported. For example, Bakkar and co-worker reported that the grain size of Al deposits clearly decreased as the electrolysis potential shifted to negative[11]. Apart from this, Wang and co-workers reported that a bright Al coating could be obtained by adding nicotinic acid or methyl nicotinate to a Lewis acidic $AlCl_3$-BMIC (1-butyl-3-methylimidazolium chloride) IL[12]. Ueda and co-workers reported that the surface roughness was improved by adding 1, 10-phenanthroline anhydrate (OP)(**Fig. 1** (a)) to a Lewis acidic $AlCl_3$-EMIC (Fig. 1 (b)) IL[14]. BASF has developed an Al deposition process using a Lewis acidic $AlCl_3$-EMIC IL with additives[20]. This process improved the adhesion and density of the Al coating. To the best of our knowledge, there are a few papers that have clearly reported the deposition rate. Instead of the deposition rate, we now focus on the relation between the current densities and current efficiencies. Kamavaram and co-workers reported that high applied voltages and concentration of $AlCl_3$ yielded high current densities[9]. In addition, the current densities obtained during this process were in the range of 200 ～ 500 Am^{-2} and the current efficiencies were in the range of 70 ～ 90%[9]. There are few articles that systematically investigated the correlation between the Al deposits and the operating conditions. In order to effectively scale up from the laboratory level to the practical level, it is desirable to make the above correlation sufficiently clear. Moreover, there are few reports that achieve both a sufficient deposition rate and smoothness at the higher current densities.

In this study, our group has focused on the Al electrolysis using room-temperature ILs. Al can easily be deposited from the chloroaluminate ILs although a practical technology for depositing Al from the ILs has still not been established. There are several problems such as a low limiting current density and deposition in a dendritic form. In particular, the high deposition rate and the smoothness of the electrolytic Al foil are required for practical application. In order to manufacture an electrolytic Al foil in the ambient temperature region, we investigated how to obtain a smooth foil at a higher current density. A Lewis acidic $AlCl_3$-EMIC melt was employed as the electrolyte, and the influence of the operating conditions, such as the operating temperature, current densities, and additives (OP), on the deposition rate and the smoothness of the electrolytic Al foil were investigated.

2. Experimental

2.1 Preparation of electrolyte

In order to remove residual moisture, anhydrous

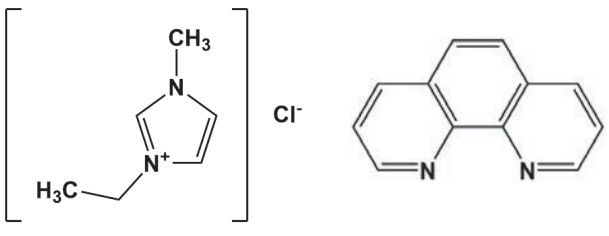

(a) (b)

Fig. 1 Structural formulas of (a) 1,10-phenanthroline anhydrate (OP) and (b) 1-ethyl-3-methylimidazolium chloride (EMIC).

$AlCl_3$ (Sigma Aldrich, ≥ 99.99%) and EMIC (Kanto Chemical Co., Inc., ≥ 98%) were dried at 60 ℃ for 10 h in vacuo. A chloroaluminate ionic liquid consisting of anhydrous $AlCl_3$ and EMIC at a 2:1 molar ratio was mixed in an Ar-filled glove box (Vacuum Atmospheres Co., VAC101965-OMNI-LAB). This ionic liquid was purified by a substitution method[21]. Al wires were immersed in the above liquid for ca 1 month, and a colorless and transparent electrolyte was obtained. 20 mmol dm^{-3} OP (Sigma Aldrich) was added to the electrolyte as an additive.

2.2 Electrochemical experiments

A constant-current electrolysis method was carried out in a conventional three-electrode cell with stirring at room temperature (RT) and 50 ℃. A Ti plate (Nilaco, thickness: 0.2 mm, purity: 99.5%) was employed as the cathode. As the pretreatment of the Ti plate, after being sonicated with ethanol and acetone, it was dried with cold air. In order to control the exposed area (0.95 cm^2) of the Ti plate to the electrolyte, it was masked with Nitoflon tape (Nitto Denko, No.903UL, thickness: 0.08 mm). A reference electrode (Al/Al(III)) was constructed by placing an Al wire (0.99-mm-diameter) in a Pyrex tube terminated with a porous G4 glass frit. The electrolyte for the reference electrode was a $AlCl_3$–EMIC melt at a 2:1 molar ratio. An Al plate (Nilaco, thickness: 1.2 mm, purity: 99.99%) was employed as the anode.

The conditions of the constant-current electrolysis were as follows: the operating temperatures of RT and 50 ℃, the stirring speed of 1500 rpm, the current density of 21.1～63.2 mA cm^{-2}, and the total charge of 30.0 C cm^{-2}. A magnetic stirrer hot plate with a stir bar of 1.5 cm long was used to control the operating temperature and the stirring speed of the electrolyte. Electrochemical experiments were performed using a computer-controlled electrochemical measuring system (Hokuto Denko, HZ-7000).

2.3 Analysis of the deposits

The surface morphology was observed using a field-emission scanning electron microscope (FE-SEM, JEOL, JSM-7001F). For observation of the crystal grains, after treating the cross section of foils with a focused ion beam processing apparatus (FIB, Hitachi High Technology, MI4050), the treated cross section was observed using a scanning ion microscope (SIM). For measurement of the foil thickness, after fixing the foil with resin, the cross-section of the foils was observed using an ultra-low accelerating voltage scanning electron microscope (ULV-SEM, JEOL Ltd., JSM-7800). The deposition rate was calculated from the foil thickness obtained from the cross-sectional SEM images and the electrolysis time for each electrolysis condition. The arithmetic mean roughness (Sa) was observed using an atomic force microscope (AFM, Park Systems, NX-10). The crystal structure was analyzed by X-ray diffraction (XRD) using an X-ray diffraction meter (Rigaku, MiniFlex600) with Cu Kα radiation (λ = 0.15418 nm). The obtained deposits were washed with ethanol and acetone to remove the electrolyte prior to analysis.

3. Results and Discussion

For the electrolytic Cu foil, it is well known that a Ti plate is used for the cathode and electrolysis is carried out at an operating temperature of 50 ℃[22]. Thus, the Al electrolysis was performed under these conditions. **Fig. 2** shows the chronopotentiograms for the depositing of Al on the Ti plate substrate under various operating conditions. These cathodic polarization curves mean the following reaction for the Al deposition.

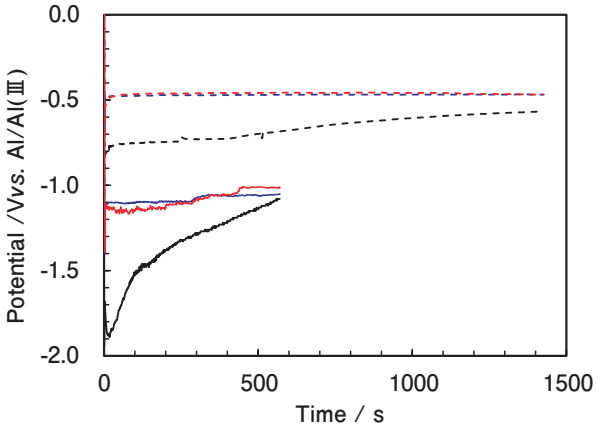

Fig. 2 Chronopotentiograms for depositing of Al on the Ti plate electrode in the $AlCl_3$-EMIC melt at (black) room temperature, (blue) 50 ℃, and (red) 50 ℃ with 20 mmol dm^{-3} of OP additive; current density: (dashed line) 21.1, (solid line) 52.6 mA cm^{-2}, total charge for all deposits: 30 C cm^{-2}.

$$4Al_2Cl_7^- + 3e^- \rightarrow Al + 7AlCl_4^- \quad [1]$$

The electrolytic potential at RT shifted negative with increasing the current density from 21.1 mA cm^{-2} to 52.5 mA cm^{-2}. Both cathodic polarization curves were measured within −2.2 V *vs.* Al / Al (Ⅲ). It has been reported that the reductive decomposition of the EMI^+ cation occurred at the potential of −2.2 V *vs.* Al / Al (III)[23]. Therefore, it is considered that no side reaction due to the reductive decomposition of the EMI^+ cation would occur. By increasing the operating temperature to 50 ℃, both electrolytic potentials at 21.1 mA cm^{-2} and 52.5 mA cm^{-2} shifted to positive. This would be because as the operating temperature increases, the specific conductivity of the electrolyte increases[24], thus the solution resistance would decrease. On the other hand, the OP addition had almost no effect on the electrolytic potential, suggesting that OP would not affect the diffusion of the reactive ion species ($Al_2Cl_7^-$ ions).

Table 1 summarizes the relation between operating conditions and current efficiencies of resulting Al foil. We defined the percent current efficiency as the ratio between the actual amount of deposits to that theoretically calculated from Faraday's laws[25]. In the OP-free bath, the current efficiencies at the operating temperature of 50 ℃ were higher than those of RT at both current densities. This would be because some of the deposit was detaching from the edge of the Ti plate substrate. Regardless of the OP addition, the current efficiencies were more than 90% even at the current density of 52.6 mA cm^{-2}, suggesting that it would be improbable to be a parasitic reaction involving OP that is competing with the Al deposition.

Fig. 3 shows the photographs of the resulting Al foil obtained on the Ti plate substrate under the various operating conditions. As shown in Fig. 3 (a), the edge of the Al foil obtained from the OP-free bath at RT was remarkably rough. As shown in Fig. 3 (b), by increasing the operating temperature, the roughness of the edge was clearly improved. As shown in Fig. 3 (c), by adding OP to the bath, a matte finish Al foil was obtained, suggesting that the smoothness would be dramatically improved by chemical action rather than by thermodynamic action (polarization effects).

Fig. 4 shows the FE-SEM images of the resulting Al foil obtained on the Ti plate substrate under the various operating conditions. The crystal grain shape was the same, like a texture, regardless of the operating conditions. As shown in Fig. 4 (a-I), (b-I), in

Table 1 Relation between operating conditions and current efficiencies of resulting Al foil.

Additives	Operating temperature ℃	Current density mA cm^{-2}	Current efficiency %
None	Room temp.	21.1	85.1
		52.6	84.8
None	50	21.1	97.5
		52.6	99.6
OP	50	21.1	95.6
		52.6	96.5

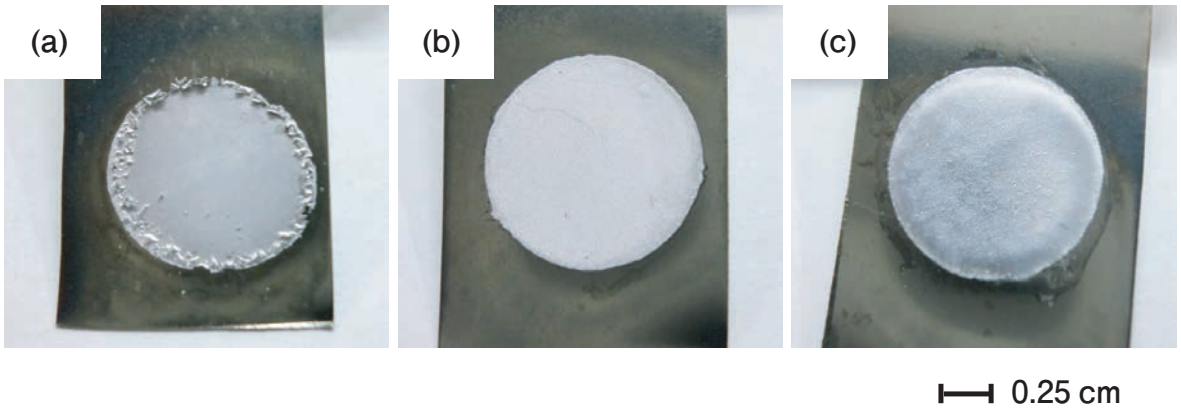

Fig. 3 Photographs of resulting Al foils obtained on the Ti plate substrate from the $AlCl_3$-EMIC melt at (a) room temperature, (b) 50 ℃, and (c) 50 ℃ with 20 mmol dm^{-3} of OP additive; current density: 42.1 mA cm^{-2}, total charge for all deposits: 30 C cm^{-2}.

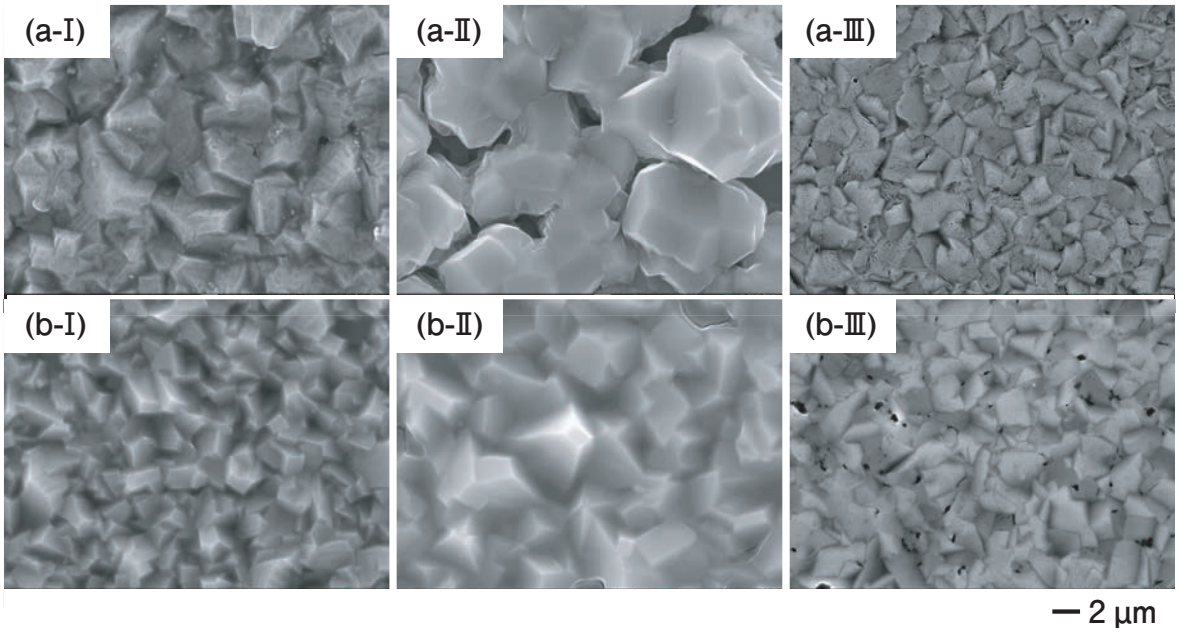

Fig. 4 FE-SEM images of resulting Al foils obtained on the Ti plate substrate from the $AlCl_3$-EMIC melt at (I) room temperature, (II) 50 ℃, and (III) 50 ℃ with 20 mmol dm^{-3} of OP additive; current density: (a) 21.1, (b) 52.6 mA cm^{-2}, total charge for all deposits: 30 C cm^{-2}.

the OP-free bath, the crystal grain size became smaller with increasing the current density. At the high current densities, many Al nuclei are generated and then each nucleus grew as the current disperses, resulting in smaller crystal grains[25, 26]. As shown in Fig. 4 (a-II), (b-II), crystal grain sizes of both samples grew larger with increasing the operating temperature. When the operating temperature increased, the surface diffusion distance of the deposited Al atoms would increase, forming large nuclei, then the current concentrates on them, resulting in the growth of large crystals[26, 27]. As shown in Fig. 4 (a-III), (b-III), at both current densities, the crystal grain size became smaller by the addition of OP. However, the addition of OP to the melt at 50 ℃ did not affect the overpotential for the electrolysis as shown in Fig. 2. This suggests that the crystal growth of Al is suppressed by the adsorption of OP itself on the substrate, similar to nicotinic acid and methyl nicotinate[12].

The effect of the operating conditions on the grain growth of the resulting Al foil was observed. **Fig. 5** shows the cross-sectional SIM images of the resulting Al foils obtained on the Ti plate substrate under the various operating conditions. Regarding the method of calculating the foil thickness, eight points were measured in the same foil, and then their average value is shown in Fig. 5. The foil thickness obtained at 50 ℃ was thicker than the foil thickness obtained at RT. This would mainly be due to the difference in the current efficiency. In the OP-free bath, the crystal grains increased and the surface roughness was high as the operating temperature increased from RT to 50 ℃. When OP was added to the bath at 50 ℃, the crystal grains were dramatically decreased and the smoothness was enhanced. Based on these SIM images, the effect of the operating temperature and the OP addition on the grain growth and the smoothness was clearly clarified.

Fig. 6 shows the AFM images and the surface roughness (Sa) values of the resulting Al foil obtained on the Ti plate substrate under the various operating conditions. As shown in Fig. 6 (a-I), (b-I), in the OP-free bath, the Sa value decreased with increasing the current density (Sa = 0.2429 μm → 0.1273 μm). As shown in Fig. 5 (a-II), (b-II), both Sa values became higher with increasing the operating temperature. Moreover, as shown in Fig. 5 (a-III), (b-III), the OP addition drastically reduced both Sa values and showed the values of about 1/10. In particular, in the case of Fig. 5 (b-III), 45.8 nm of Sa was obtained, which was smoother than the Sa value (105.8 nm) of the commercial Al foil for a battery current collector. By adding OP to the melt, the Sa value became

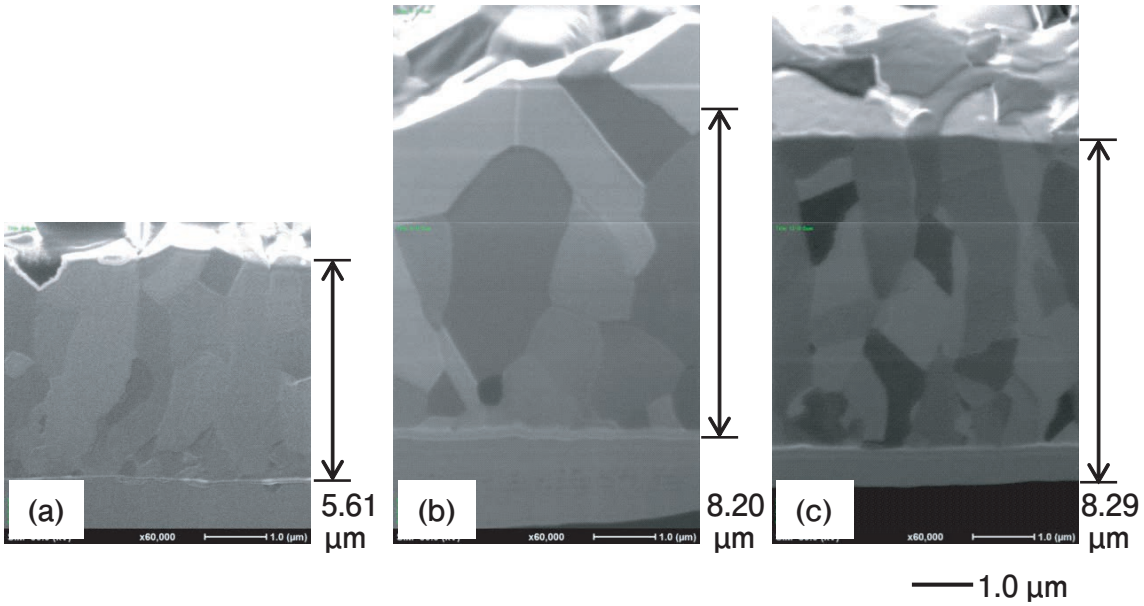

Fig. 5 Cross-sectional SIM images of resulting Al foils obtained on the Ti plate substrate from the $AlCl_3$-EMIC melt at (a) room temperature, (b) 50 ℃, and (c) 50 ℃ with 20 mmol dm^{-3} of OP additive; current density: 52.6 mA cm^{-2}, total charge for all deposits: 30 C cm^{-2}.

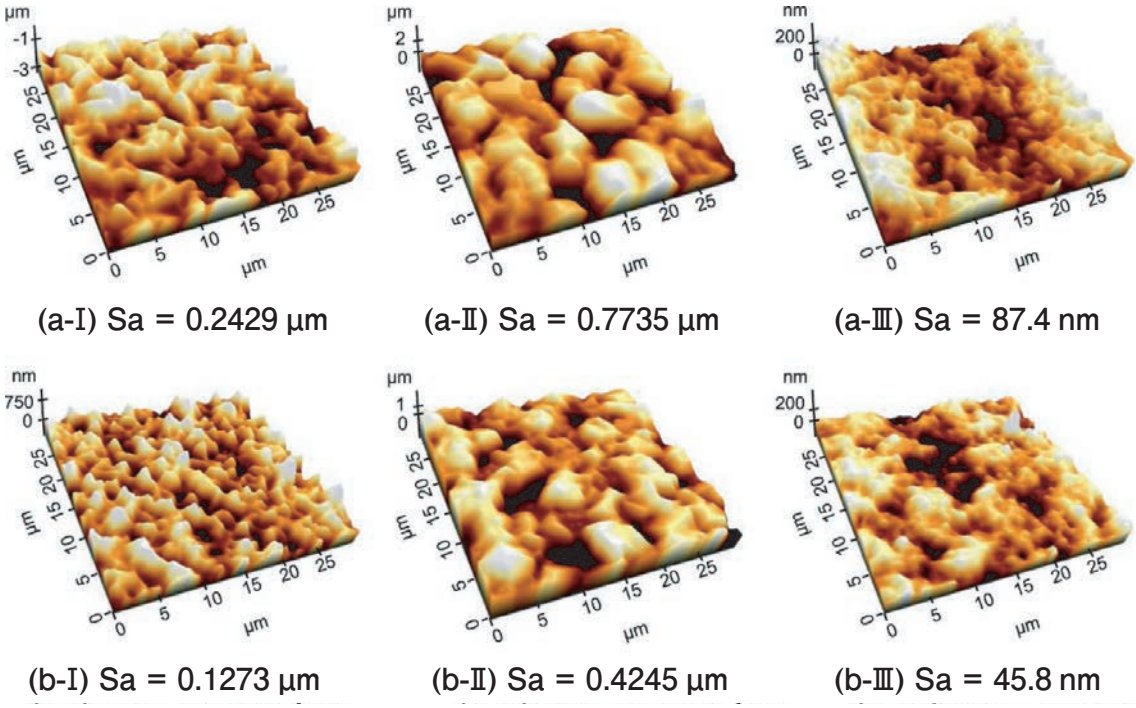

Fig. 6 AFM images of resulting Al foils obtained on the Ti plate substrate from the $AlCl_3$-EMIC melt at (I) room temperature, (II) 50 ℃, and (III) 50 ℃ with 20 mmol dm^{-3} of OP additive; current density: (a) 21.1, (b) 52.6 mA cm^{-2}, total charge for all deposits: 30 C cm^{-2}.

significantly lower, indicating that the OP addition strongly suppresses the roughness. These results are consistent with the trend in the crystal grain sizes shown in Fig. 4.

Fig. 7 shows the relation between the current density and the deposition rate calculated from the foil thickness obtained from the cross-sectional SEM image (not shown). As the current density increased, the deposition rate increased. Further increasing the operating temperature significantly increased the deposition rate. This would be because the current efficiency increased due to the increase in the operating temperature. A linear relation was shown with or without OP although the linear relation was lost at the current density of 52.6 mA cm^{-2} or higher. This is due to the decrease in the foil thickness due to

the decrease in current efficiency. At the operating temperature of 50 ℃ and current density of 52.5 mA cm^{-2}, the deposition rates of the OP-free bath and the OP-added bath were 0.863 μm min^{-1} and 0.872 μm min^{-1}, respectively. The OP addition had almost no effect on the deposition rate. This would be because OP does not affect the diffusion of the $Al_2Cl_7^-$ ions.

Fig. 8 shows the XRD patterns of the resulting Al foil obtained on the Ti plate substrate under the various operating conditions. The XRD peaks were identified and indexed by the comparison to the standard obtained from the JCPDS card (#04-0787). All the peaks were attributed to Al (fcc), thus the single phase was obtained. In the OP-free bath, the (200) reflection became strong as the operating temperature was high. Moreover, the orientation of the (200) reflection was strong due to the OP addition. This result is similar to the previously reported preferential orientation of the (200) plane and bright coatings with additives[12, 14, 28]. Based on the (200) reflection of the XRD patterns, the crystallite sizes were calculated using Scherrer's equation:

$$D = K\lambda / \beta \cos\theta \quad [2]$$

where D is the crystallite size (nm); K is the Scherrer constant (0.9); λ is the X-ray wavelength (0.15418 nm); β is Full Width of Half Maximum (FWHM, rad); and θ is the Bragg angle. The relation between the operating conditions and crystallite size of the resulting Al foil is listed in **Table 2**. The crystallite size became small with increasing the current density. By increasing the operating temperature, both crystallite sizes increased. Moreover, both crystallite sizes were dramatically decreased by the OP addition.

The current density and the operating temperature are closely related to the electrolytic potential[19], so it is considered that the factor that determines the crystallite sizes is the electrolytic potential. **Fig. 9** shows the relation between the electrolytic potential and crystallite size of the resulting Al foils obtained on the Ti plate substrate under the various operating conditions. In fact, when the relation between the electrolytic potential and the crystallite size was plotted, a proportional relation was clearly demonstrated. In the OP-free bath, it is suggested that the crystallite size depends on the overpotential rather than the operating temperature. By increasing the operating temperature, the surface roughness became higher and the crystallite size grew.

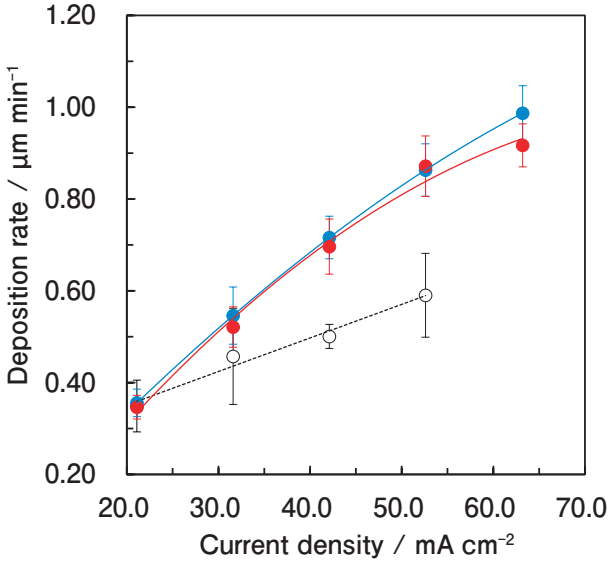

Fig. 7 Relation between the current density and the deposition rate of resulting Al foils obtained from the $AlCl_3$-EMIC melt at (black) room temperature, (blue) 50 ℃, and (red) 50 ℃ with 20 mmol dm^{-3} of OP additive.

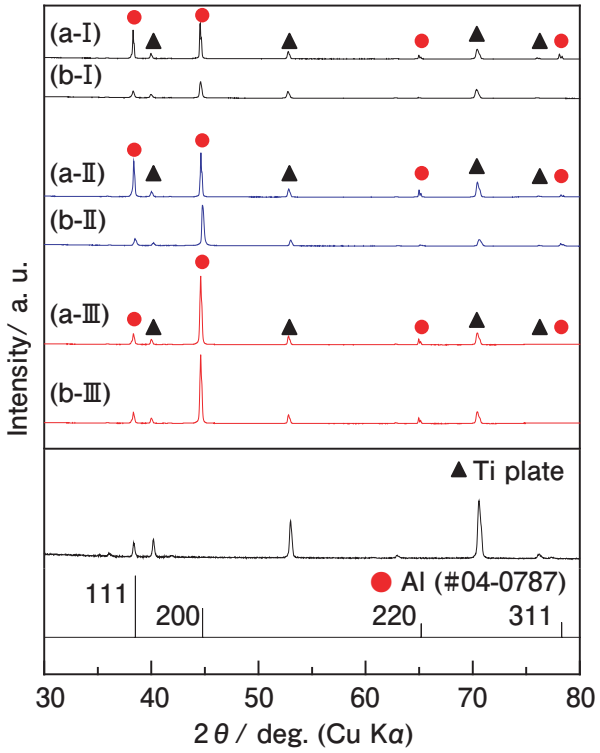

Fig. 8 XRD patterns of resulting Al foils obtained on the Ti plate substrate from the $AlCl_3$-EMIC melt at (I) room temperature, (II) 50 ℃, and (III) 50 ℃ with 20 mmol dm^{-3} of OP additive; current density: (a) 21.1, (b) 52.6 mA cm^{-2}, total charge for all deposits: 30 C cm^{-2}.

Table 2 Relation between operating conditions and crystallite size of resulting Al foil (XRD).

Additives	Operating temperature ℃	Current density mA cm^{-2}	Crystallite size nm
None	Room temp.	21.1	80.1
		52.6	75.4
None	50	21.1	90.0
		52.6	78.3
OP	50	21.1	70.3
		52.6	49.3

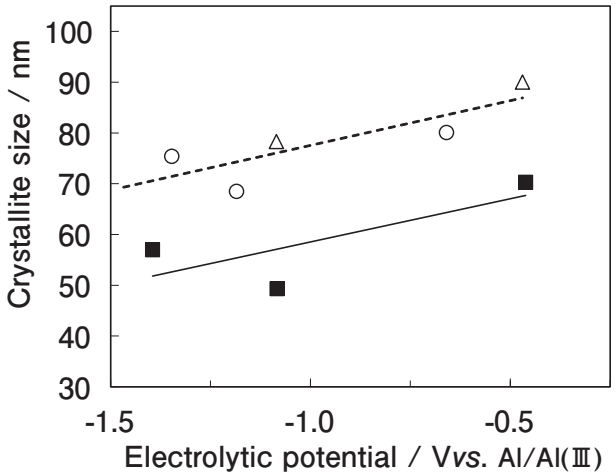

Fig. 9 Relation between the electrolytic potential and crystallite size of resulting Al foils obtained on the Ti plate substrate from the $AlCl_3$-EMIC melt at (○) room temperature, (△) 50 ℃, and (■) 50 ℃ with 20 mmol dm^{-3} of OP additive; total charge for all deposits: 30 C cm^{-2}.

Therefore, when OP was added to the electrolyte at the operating temperature of 50 ℃, OP exhibited the effect of improving the surface roughness without affecting the electrolytic potential. While no luster was observed in the resulting Al foil obtained from the OP-free bath, the matte finish surface was observed in the resulting Al foil obtained from the OP-added bath, independent of the current density (21.1～63.2 mA cm^{-2}). Based on these results, it was clarified that the grain size and the crystallite size of the resulting Al foil were reduced by the OP addition, which improved the surface roughness regardless of the overpotential.

4. Conclusions

We investigated the influence of the operating conditions, such as operating temperature, current densities, and additives (1,10-phenanthroline anhydrate, OP), on the surface roughness (smoothness) and the deposition rate of electrolytic Al foil, and the following results were obtained. By increasing the operating temperature to 50 ℃, the overpotential decreased, and even at a high current density, the electrolysis became possible without reaching the cathode limit potential of −2.2 V *vs.* Al/Al(III). The AFM image revealed that the surface roughness (Sa) value of the electrolytic Al foil obtained from the $AlCl_3$-EMIC melt with the OP additive at 50 ℃ was 45.8 nm at the current density of 52.6 mA cm^{-2}. The smooth electrolytic Al foil was successfully obtained even with a high operating temperature and high current density by adding OP to the melt. Although the deposition rate increased with increasing the operating temperature to 50 ℃, the OP addition had little influence on the deposition rate. At the operating temperature of 50 ℃ and the current density of 52.6 mA cm^{-2} or lower, the current efficiencies were 90% or more. At the current density of 52.6 mA cm^{-2}, the deposition rate was about 0.9 μm min^{-1} regardless of the OP addition. The OP addition reduced the grain size and improved the smoothness. The crystallite size was affected by the OP addition rather than the overpotential. In conclusion, the operating temperature needs to be increased to enhance the deposition rate and achieve a current efficiency of 90% or more, and the OP addition is significantly necessary to enhance the smoothness.

Acknowledgment

This work is based on results obtained from a project commissioned by the New Energy and Industrial Technology Development Organization (NEDO).

REFERENCES

1) H. Matsuoka and N. Higashi: J. Jpn. Inst. Light Met., **67** (2017), 641-652.
2) A. Okamoto, M. Morita, and N. Yoshimoto: J. Surf. Finish.

Soc. Jpn., **63** (2012), 641-645.
3) A. Okamoto, N. Niwa, M. Egashira, M. Morita, and N. Yoshimoto: Electrochemistry, **81** (2013), 906-911.
4) S. Takahashi, K. Akimoto, and I. Saeki: J. Surf. Finish. Soc. Jpn., **40** (1989), 548-552.
5) L. Qingfeng, H. A. Hjuler, R. W. Berg, and N. J. Bjerrum: J. Electrochem. Soc., **137** (1990), 593-598.
6) Q. Liao, W. R. Pitner, G. Stewart, C. L. Hussey, and G. R. Stafford: J. Electrochem. Soc., **144** (1997), 936-943.
7) Y. Zhao and T. J. VanderNoot: Electrochim. Acta., **42** (1997), 1639-1643.
8) C. A. Zell, F. Endres, and W. Freyland: Phys. Chem. Chem. Phys., **1** (1999), 697-704.
9) V. Kamavaram, D. Mantha, and R. G. Reddy: Electrochim. Acta., **50** (2005), 3286-3295.
10) Q. X. Liu, S. Zein El Abedin, and F. Endres, Surf. Coat. Technol., **201** (2006), 1352-1356.
11) A. Bakkar and V. Neubert, Electrochim. Acta., **103** (2013), 211-218.
12) Q. Wang, Q. Zhang, B. Chen, X. Lu, and S. Zhang: J. Electrochem. Soc., **162** (2015), D320-D324.
13) H. Takahashi, H. Matsushima, and M. Ueda: J. Electrochem. Soc., **164** (2017), H5165-H5168.
14) H. Takahashi, C. Namekata, T. Kikuchi, H. Matsushima, and M. Ueda: J. Surf. Finish. Soc. Jpn., **68** (2017), 208-212.
15) T. Hirato, J. Fransaer, and J.-P. Celis: J. Electrochem. Soc., **148** (2001), C280-C283.
16) M. Li, B. Gao, C. Liu, W. Chen, Z. Shi, X. Hu, and Z. Wang: Electrochim. Acta., **180** (2015), 811-814.
17) E. Rodríguez-Clemente, T. L. Manh, C. E. Guinto-Pano, M. Romero-Romo, I. Mejía-Caballero, P. Morales-Gil, E. Palacios-González, M. T. Ramírez-Silva, and M. Palomar-Pardavé: J. Electrochem. Soc., **166** (2019), D3035-D3041.
18) J. Miyake: J. JIEP, **6** (2003), 528-533.
19) M. Paunovic and M. Schlesinger: Fundamentals of Electrochemical Deposition, John Wiley & Sons, , New York, NY (1998), 249.
20) M. O' Meara, A. Alemany, M. Maase, U. Vagt, and I. Malkowsky: Metal Finishing, **107** (2009), 38-39.
21) S. Takahashi and N. Koura: J. Electroanal. Chem., **188** (1985), 245-255.
22) I. Shitanda, T. Ono, M. Itagaki, K. Watanabe, N. Koura, and T. Yamaguchi: J. Surf. Finish. Soc. Jpn., **60** (2009), 56.
23) M. Lipsztain and R. A. Osteryoung: J. Electrochem. Soc., **130** (1983), 1968-1969.
24) A. A. Fannin, Jr., D. A. Floreani, L. A. King, J. S. Landers, B. J. Piersma, D. J. Stech, R. L. Vaughn, J. S. Wilkes, and J. L. Williams: J. Phys. Chem., **88** (1984), 2614-2621.
25) M. Paunovic and M. Schlesinger: Fundamentals of Electrochemical Deposition, John Wiley & Sons, New York, NY (1998), 198.
26) T. Watanabe: Metals, **66** (2002), 339-349.
27) T. Watanabe: Metals, **66** (2002), 350-361.
28) X. Fang, K. Uehara, S. Kaneko, S. Sato, T. Tanabe, T. Gunji, and F. Mathumoto: Electrochemistry, **84** (2016), 17-24.

Koichi Ui
Faculty of Science and Engineering,
Iwate University,
Dr. Eng.

Satoshi Kobayashi
Nippon Light Metal Company, Ltd.
Formerly Graduate School of Engineering,
Iwate University.

Kuniaki Sasaki
Technical Division, Iwate University.

Tatsuya Takeguchi
Faculty of Science and Engineering,
Iwate University,
Dr. Eng.

Tetsuya Tsuda
Faculty of Engineering, Chiba University,
Dr. Energy Science.

Mikito Ueda
Faculty of Engineering, Hokkaido University,
Dr. Eng.

Junji Nunomura
Research Department I,
Research & Development Center,
Marketing & Technology Division,
UACJ Corporation/Faculty of Engineering,
Hokkaido University.

Yukio Honkawa
Climate Change Task Force Department,
Corporate Sustainability Division,
UACJ Corporation.

Yoichi Kojima
Research & Development Center,
Marketing & Technology Division,
UACJ Corporation,
Ph. D.